Taylor & Francis
Taylor & Francis Group

Cell Adhesion & Migration

ISSN: 1933-6918 (Print) 1933-6926 (Online) Journal homepage: http://www.tandfonline.com/loi/kcam20

Boyden chamber-based method for characterizing the distribution of adhesions and cytoskeletal structure in HT1080 fibrosarcoma cells

József Tóvári, Krisztina Futosi, Alexandra Bartal, Enikő Tátrai, Alexandra Gacs, István Kenessey & Sándor Paku

To cite this article: József Tóvári, Krisztina Futosi, Alexandra Bartal, Enikő Tátrai, Alexandra Gacs, István Kenessey & Sándor Paku (2014) Boyden chamber-based method for characterizing the distribution of adhesions and cytoskeletal structure in HT1080 fibrosarcoma cells, Cell Adhesion & Migration, 8:5, 509-516, DOI: 10.4161/cam.28734

To link to this article: http://dx.doi.org/10.4161/cam.28734

RESEARCH PAPER

Cell Adhesion & Migration 8:5, 509–516; September/October 2014; © 2014 Taylor & Francis Group, LLC

Boyden chamber-based method for characterizing the distribution of adhesions and cytoskeletal structure in HT1080 fibrosarcoma cells

József Tóvári[1,*], Krisztina Futosi[1], Alexandra Bartal[1,2], Enikő Tátrai[1], Alexandra Gacs[1], István Kenessey[3], and Sándor Paku[4]

[1]Department of Experimental Pharmacology; National Institute of Oncology; Budapest, Hungary; [2]Department of Central Pharmacy; National Institute of Oncology; Budapest, Hungary; [3]2nd Department of Pathology; Semmelweis University; Budapest, Hungary; [4]1st Department of Pathology and Experimental Cancer Research; Semmelweis University; Budapest, Hungary

Keywords: cell migration, fibroblast-type motility, Boyden chamber, migration assay, adhesion plaque dynamics

Abbreviations: 2D, two-dimensional; 3D, three-dimensional; ECM, extracellular matrix; GRE, graded radial extension; HMM, heavy meromyosin.

A 2D model was previously presented that describes the gliding motility of human fibrosarcoma cells. The model was based on the observation that adhesions are present only on the outer rim of the leading lamella of the semicircular cell. The present model describes the organization of adhesions and the cytoskeleton of migrating HT1080 fibrosarcoma and LX2 hepatic stellate cells in three dimensions. The migration assays were performed in a modified Boyden chamber using fibronectin, Matrigel, or collagen I as chemoattractants. The distribution of the adhesions was analyzed by confocal laser scanning microscope, and following decoration with heavy meromyosin, the organization of actin filaments was analyzed by electron microscopy. Double labeling was performed to study the relationship of the actin and vimentin filament network in the moving cells. Vinculin containing adhesions were observed only at the front of the cell in the form of a ring while passing through a filter pore of the Boyden chamber. Actin filaments were present only below the plasma membrane, except the very tip of the leading lamella. Vimentin intermediate filaments were localized around the cell nucleus behind the actin filament-rich lamella.

This paper describes a model of the organization of adhesions and the cytoskeleton of migrating cells in the Boyden chamber. The model is based on the observation that adhesions are present only at the leading edge of the cell. The results extend the earlier 2D model of cell locomotion into 3D.

Introduction

Cell migration in vivo and in vitro takes place within or on the surface of extracellular matrix (ECM). The advancing lamella must adhere to a variety of matrix elements to generate traction forces for motion. The force is exerted by the actin filaments of the cytoskeleton that are linked indirectly through the membrane to the substrate. Actin recruitment to the cytoplasmic domain of integrins, the formation of focal complexes occurs in collaboration with different cytoskeletal proteins including talin, vinculin, α-actinin, paxillin, zyxin, VASP, FAK, p130Cas.[1]

The locomotion of fibroblasts and fish epidermal keratocytes are probably the most intensively studied model systems.[2-5] The main differences between these two types of migration are the shape of the cells along with the distribution of adhesion sites and actin filaments during the movement. Keratocytes move rapidly showing a semicircular shape, and their long axis is perpendicular to the direction of movement.[6,7] Their motility is described by the graded radial extension (GRE) model, assuming that all points of the cell edge move perpendicularly to the semicircular lamella following a curved path with respect to the substrate.[6] The adhesions are stationary with respect to the substrate and connected by actin cables perpendicular to the direction of migration.[6] In the model describing the motion of fibroblasts, the long axis of cells and the force-generating actin bundles are parallel to the direction of movement. The cells move slowly, and their movement can be divided to three distinct steps: extension of the leading lamella is followed by cell body translocation and tail retraction.[8,9] The adhesions are located under the whole body of the cells and the actin cables connecting them are robust. Although HT1080 human fibrosarcoma cells are of fibroblast origin, their shape during movement on Matrigel-coated planar surfaces is similar to that of fish keratocytes, and their speed is surprisingly high compared with other tumor cells. Based on

*Correspondence to: József Tóvári; Email: tozsi@oncol.hu or jtovari@yahoo.com
Submitted: 01/21/2014; Revised: 03/28/2014; Accepted: 04/01/2014
http://dx.doi.org/10.4161/cam.28734

these observations, we previously have presented a model that predicts the path of the adhesion points during movement.[10] Discrete adhesion points are formed only at the edge of the semicircularly shaped lamella in a discontinuous manner as the edge moves forward but overall in time they follow a curved path in relation to the substrate, according to the GRE model.[6] As adhesions move clockwise and counterclockwise on the two sides of the apex of the cell, the connecting actin arcs grow in length as they move backward with respect to the cell. At the long axis of the cell, the adhesions at both ends of the actin cables are disintegrated resulting in the disassembly of the actin cables connecting them. Several different chemotactic assays are used to investigate tumor cell motility in vitro. The above described model was based on a 2D model system that yields insufficient information. New techniques were explored for 3D investigations.[11] Among those, the sophisticated 3D ex vivo system developed by Tayalia and colleagues allows for studying the interplay of both chemokine gradient and ECM architecture in directed migration.[11]

The authors of the present paper examined the fate of adhesion points and the arrangement of cytoskeletal components within a 3D system. Adhesion points were observed exclusively as a ring at the leading edge of the cells passing through the filter pore of the Boyden chamber. The diameter of the ring increased gradually as the cell spread over the bottom side of the filter. Actin filaments were located directly under the plasma membrane within the pore and forming arcs the ends of which were attached to the adhesion points as the cell spread over the filter. Intermedier filaments (vimentin) enwrapping the nucleus moved behind the actin filaments.

These findings support and extend our earlier model that describes the adhesion plaque dynamics and cytoskeletal arrangement in 2D migration.

Results

In vitro 3D system

In the present work, we examined the fate of adhesions and cytoskeletal elements in migrating cells through three-dimensional pores using the Boyden chamber. The experiments were terminated at different time points to analyze all stages of the migration process through the membrane. Immunofluorescent labeling was performed, followed by 3D reconstruction of the adhesion points within the pore, using confocal microscopy. The structure of the actin cytoskeleton was examined in HT1080 tumor cells after the cells reached the bottom side of the filter as it could not be reconstructed within the pore using the above described method.

Adhesions

Overall view of the bottom side of the filter (at 30 min of migration) revealed numerous circularly arranged vinculin-containing adhesions, showing differences in fluorescence intensity representing a HT1080 human fibrosarcoma cell at different stages of the migration process using fibronectin as chemoattractant (**Fig. 1A**). Similarly to the two-dimensional system, we observed adhesions exclusively at the leading edge of the migrating cells, no other adhesions were present in the pore. The tail of the cell lacking adhesions floated freely in the medium of the upper chamber (**Fig. 1B**, arrow). Occasionally, adhesions could be observed also on the upper surface of the filter. The shape of the adhesions varied at different stages of the locomotion through the filter. Adhesions at the front of the cells within the pore looked like small dots. They increased in size and became elongated when the cells reached the bottom surface of the filter (**Fig. 1C and D**). Similar distribution and structure of adhesions in HT1080 tumor cells were observed when Matrigel or collagen I were used as chemoattractant (**Fig. 2A–F**), or during the migration of the non-tumorous LX2 human hepatic stellate cell line against fibronectin (**Fig. 2G–J**).

Adhesions and actin filaments

The intense vinculin-containing adhesions arranged as a definite line at the leading edge of the cells within the pore (viewed from the side) were associated with a somewhat broader intense band of filamentous actin. The cell body within the pore showed only faint actin staining while the trailing edge of the cells located on the top of the filter contained actin filaments even in the part of the cell body not attached to the filter (**Fig. 3A and B**).

In cells at the edge of the bottom side of the pore (viewed from the bottom) actin filaments were not arranged as structured bundles and actin staining at some places reached over the adhesions, suggesting that the membrane protrudes actively during migration (**Fig. 3C1**). As the cells pushed forward and the area occupied increased, the shape of adhesions became elongated and the actin filament bundles began to form arcs and organize into cables (**Fig. 3C2–4**). These arcs closely resemble the arcs formed during regular spreading over Matrigel-coated glass surface (**Fig. 3D**).

Heavy meromyosin (HMM) decoration

To reveal the organization of the actin bundles at front and especially in the cell body within the pore, HMM decoration was performed. At all stages of the migration actin filaments were observed exclusively beneath the membrane (except the very tip of the advancing lamella) (**Fig. 4**). The thickness of the layer formed by the actin filaments was the smallest in the cell body within the pore (~0.2 μm, **Fig. 4D–G**). However, the most distant parts of cell protrusions were filled (1–2 μm) with actin filaments (**Fig. 4C, H, and I**). At no part of the migrating cells could preferential filament polarity be observed (not shown).

Actin and vimentin

We examined the co-localization of actin bundles and vimentin filaments during 2D and 3D migration of tumor cells, as well. Double labeling was performed to study the relationship of the actin and vimentin filament network. 2D analysis of the moving cells showed that the vimentin intermediate filaments were localized around the cell nucleus (**Fig. 5A**). A similar arrangement can be observed in the 3D model system: the vimentin filament network advanced behind the actin filament-rich lamella (**Fig. 5B**).

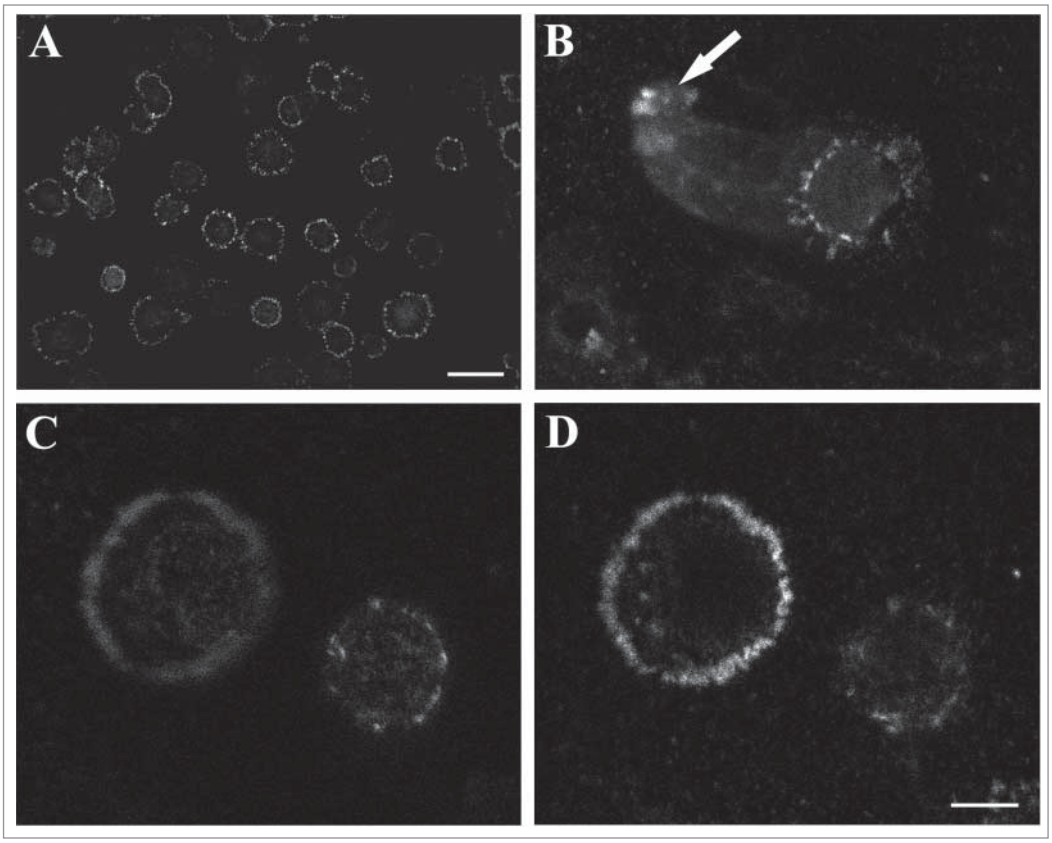

Figure 1. (**A**) Overview of the bottom side of the filter. Numerous circularly arranged, vinculin-containing adhesions are observed which represent cells at different stages of the migration process. The circles with the smallest diameter show cells in pores just reaching the bottom surface of the filter. Scale bar: (**A**) 20 μm. (**B**) Horizontal view of a cell passing through a pore reconstructed from 30 (~30 μm) optical sections. The cell just reached the bottom side of the filter. Note that only the very front of the cell contains adhesion plaques and no other adhesions are present in the pore. The tail of the cell floats freely in the medium of the upper chamber (arrow). (**C and D**) Two optical sections at 2 μm distance of two cells in different stages of migration through the filter. The cell on the right is still in the pore and has a small dot-like adhesion at its front. The cell on the left already reached the bottom surface of the filter and starts to spread exhibiting elongated adhesions. Scale bar: (**B–D**) 5 μm.

Discussion

Tumor cell motility is influenced by various factors. The elucidation of migratory properties and the development of model systems are subjects of intense research. Three-dimensional assays have been postulated to be more biologically relevant than 2D assays.[12] Cell migration is coordinated by proteins localized to focal adhesions.[13] Vinculin, a regulatory adaptor protein, has a pivotal role in the organization of adhesion sites during cell locomotion.[14,15] Vinculin interacts directly with talin and actin connecting actin filaments to the adhesions.[16] Vinculin contributes to increasing the generation of contractile forces via integrin receptors, and thus, has been suggested to facilitate 3D cell invasion.[17] Vinculin is detected at the matrix contact sites of migrating cells in 3D collagen matrices and co-localized with beta1-integrin, focal adhesion kinase (FAK), and filamentous actin.[12] Using Fourier transform traction microscopy in their assays, Mierke and coworkers proposed that vinculin-mediated enhanced contractility contributes to the ability of tumor cells to overcome the steric hindrance of 3D ECMs during invasion.[18] Their results suggest that an important regulatory role may be attributed to vinculin in cell motility within 3D ECM and in metastasis formation.

Based on the cell type, arrangement of actin arcs may differ in pattern during movement and so do traction forces exerted by focal adhesions, depending on their precise localization within the cell.[19] Previous data suggest that, in contrast to cell migration in 2D, the traction forces in 3D gels are transmitted through the randomly distributed attachments between cell and matrix present over the entire surface of both spindle-shaped and amoeboid moving cells.[20,21] Tumor cells in vivo were observed to extend F-actin-rich protrusions forward and adhere to their surroundings, followed by contraction of the trailing end (motility cycle).[22]

The present model of the organization of adhesions and the cytoskeleton of stimulated migrating cells in Boyden chamber (**Fig. 6**) supplements an earlier model describing the locomotion of cells on planar surfaces.[10] Both models are based on the observation that adhesions are present only at the leading edge of the cell. This manifests as a ring of adhesions at the front of the cells in the pore of the migration filter in the simple 3D system used. The latter seems to be a general phenomenon as the arrangement of the adhesions were independent of the cell line, and the chemoattractant used. In two dimensions, the cell has a semicircular shape and the adhesions are located on the circumference of the semicircle. Both arrangements exclude the possibility that actin cables are oriented parallel to the direction of migration. This statement is also supported by the observation that the orientation of the actin arcs is parallel to the membrane within the cells that have already reached the bottom side of the filter. Accordingly, no actin cables were detected which run perpendicular to the circular cell periphery toward and/or entering the pore. As the cells at this stage of migration undergo spreading at the bottom side of the filter, the arrangement of the actin arcs is identical to the actin arcs present in cells spreading over planar surfaces.

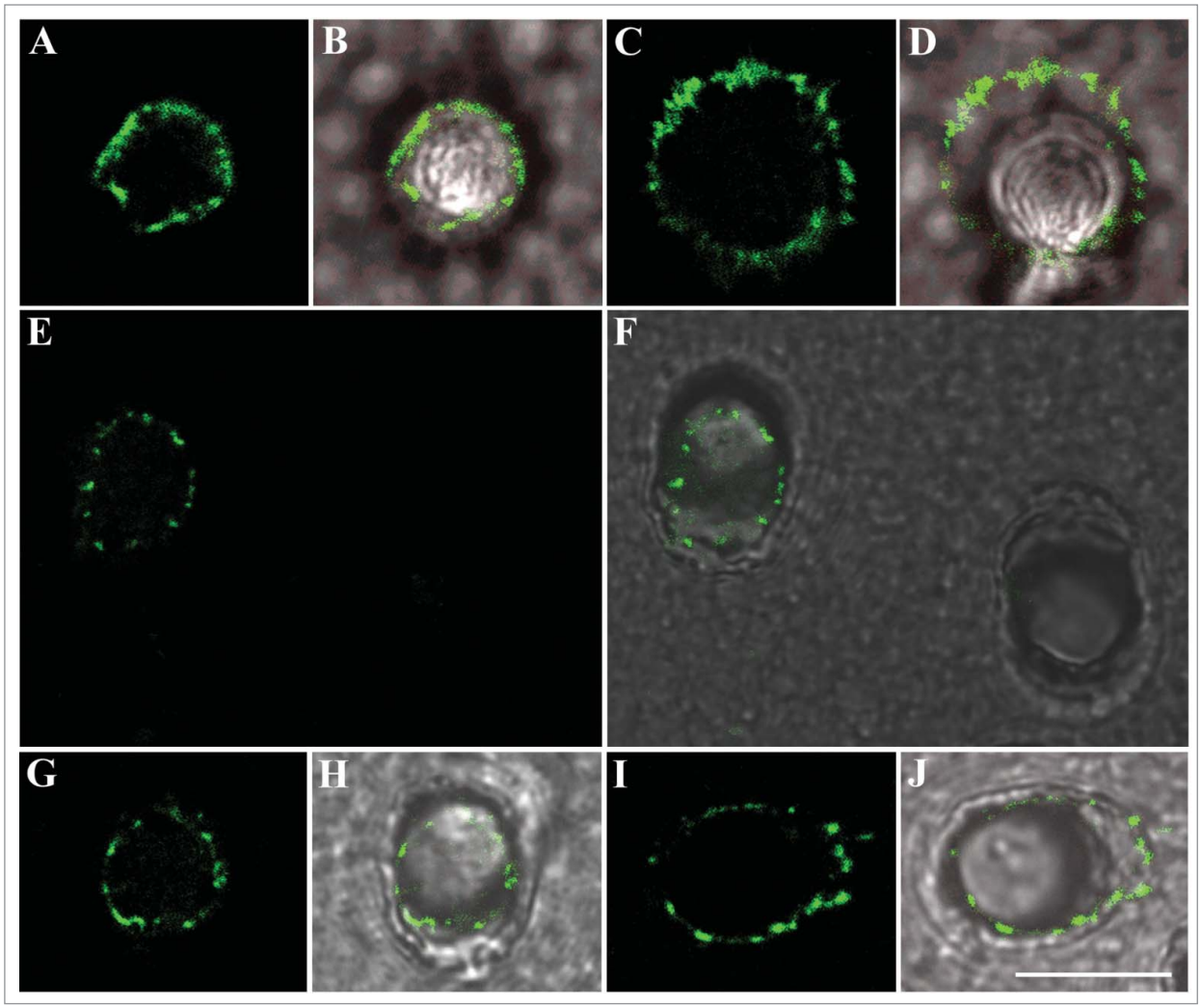

Figure 2. (**A–F**) Distribution of adhesions in HT1080 tumor cells migrating through the pores of the Boyden chamber toward Matrigel (**A–D**) and collagen I (**E and F**). Note that, on both matrices, the adhesions are arranged in a circular manner. (**A and B**) Show a cell with the pore, (**C and D**) show a cell already passed the brim of the pore. (**A, C, and E**) Show the immunofluorescence, (**B, D, and F**) show the merged image of immunofluorescence, and phase contrast. At the lower right are of **Figure 2F** a pore is visible without cell. (**G–J**) Distribution of adhesions in LX2 cells migrating through the pores of the Boyden chamber toward fibronectin. Note that, at the front of migrating cells, the adhesions are arranged in a circular manner. (**G and H**) Show a cell within the pore, (**I and J**) show a cell already passed the brim of the pore. (**G and I**) Show the immunofluorescence, (**H and J**) show the merged image of immunofluorescence, and phase contrast. Scale bar: 10 μm.

Continuous movement in two and three dimensions and spreading with a steady speed are enabled through the described orientation of the actin arcs. The authors were not able to resolve the structure of the actin filaments within the pore, but the early appearance of the arcs as the cells reach the bottom surface of the filter makes it plausible that these structures are already present within the pore in an immature form. The arcs together with their adhesions are produced continuously at the leading edge of the cell under all three conditions (2D, 3D migration, spreading). The structure of the actin machinery (arc) is responsible for cell body translocation and spreading. The arcs are created either by the tethering force of the nucleus enwrapped in the vimentin network, which is coupled to the actin cytoskeleton during the two- and three-dimensional migrations, or by the counterbalancing force of the contractile actin cables present at the whole circumference of the cells in many directions while spreading. The arcs composed of alternating polarity actin filaments are under tension and would straighten without an equally high counterforce.[9] The asymmetric arrangement of the arcs during two- and three-dimensional movement leads to cell body translocation, in contrast to spreading where the arcs are present at the whole circumference of the cell thereby are in balance. The forces of the arcs during spreading stabilize the location of the nucleus and other cell organelles. The dynamics of the adhesions in 2D correspond very well with the predictions of the GRE model (the adhesions are renewed continuously at the end of the actin arcs and move on a curved path in time, and the size of the cell remains constant).[7] During spreading, as the area covered by the cells grows steadily, the adhesions should move on a straight line in a radial direction.

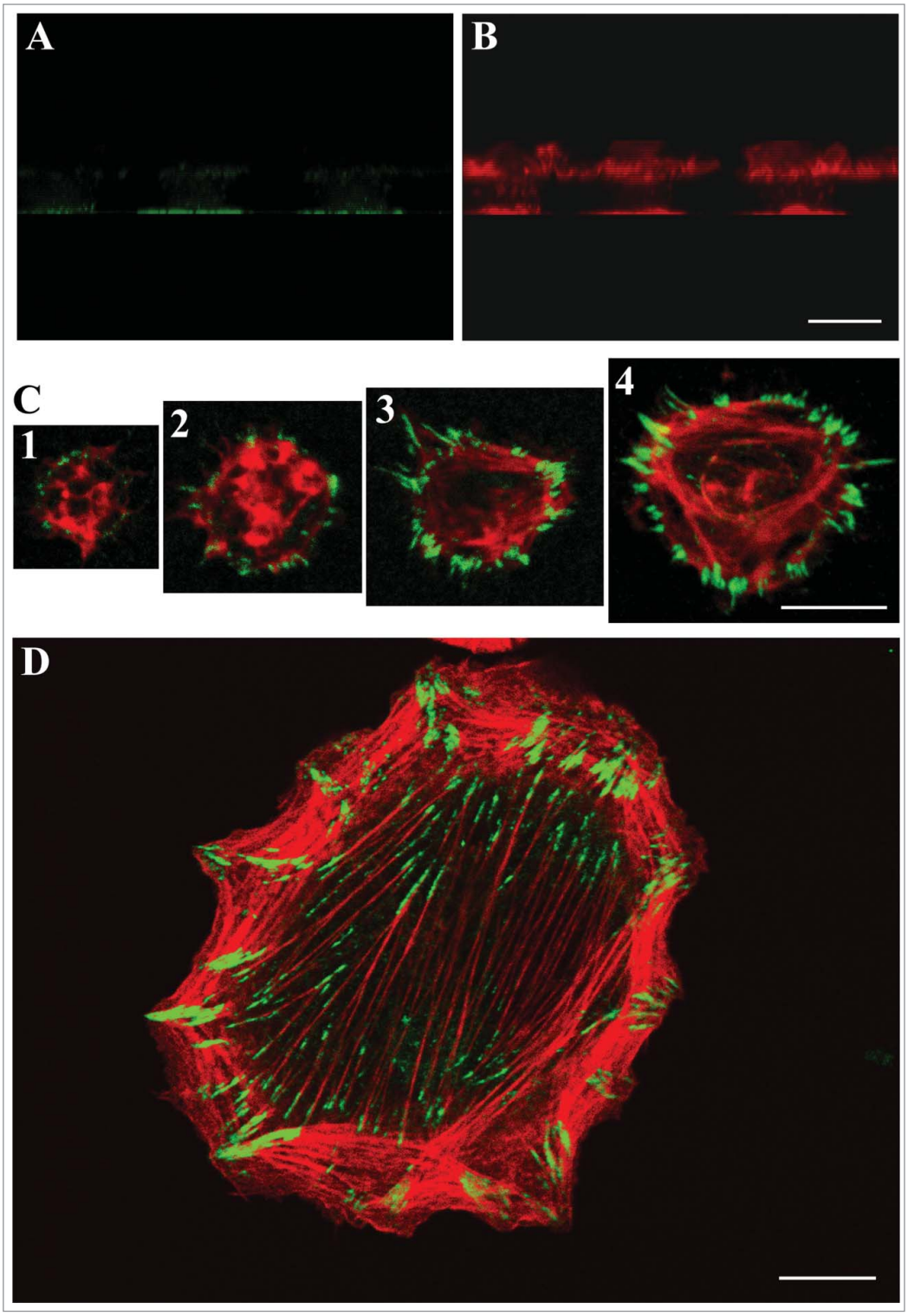

Figure 3. (**A and B**) Side view of three cells migrating through the filter reconstructed from 28 (~20 μm) optical sections. The filter was double-labeled for vinculin (**A**) and filamentous actin (**B**). The vast majority of the adhesions are located at the front of the cells. The front of the cell on the left is still within the pore. Actin filaments are concentrated at the front side and on the top of the filter. The enrichment of the actin filaments can also be the consequence of the increased width of the cell at the later location. The bodies of the cells are also visible above the top of the filter. (**C**) Bottom view of the filter showing cells at different stages of the migration process. Double labeling for vinculin (green) and filamentous actin (red). (**C1**) Cell on the edge of the pore. The dot-like, vinculin-containing adhesions are arranged in a circular manner. No organized actin cables are visible. Note that actin-containing cellular processes reach over the adhesions. (**C2**) Elongated vinculin-containing adhesions are visible at the front of the cell that is moving out from the pore, but actin cables are not formed. (**C3**) Moving cell in a similar position as in **C2**. The adhesions are more elongated and actin filaments are more organized. (**C4**) Cell in an advanced stage of the passage through the filter. Note that actin cables forming arcs connect the elongated vinculin-containing adhesion plaques. No actin cables traverse through the cell over the pore. (**D**) A fully spread HT1080 cell on Matrigel-coated glass surface. The peripheral actin filaments are arranged in arcs, in a similar manner observable in the cell depicted in **C4**. The actin cables traversing the center represent straightened arcs leftover from a previous spreading stage. Scale bars: (**A–D**) 10 μm.

Materials and Methods

Tumor cells and culture conditions

The human fibrosarcoma HT1080 cells were maintained in RPMI 1640 tissue culture medium (Sigma Chemical Co.) supplemented with 10% fetal calf serum (FCS, Sigma) and 1% penicillin-streptomycin (PS, Sigma). The LX2 spontaneously immortalized human hepatic stellate cell line was used as non-tumorous control.[23,24] These cells were maintained in Dulbecco's modified Eagle's medium (DMEM) supplemented with 10% FCS, 1% penicillin-streptomycin (PS, Sigma). All cells were kept in an incubator providing humid atmosphere of 5% CO_2 at 37°C.

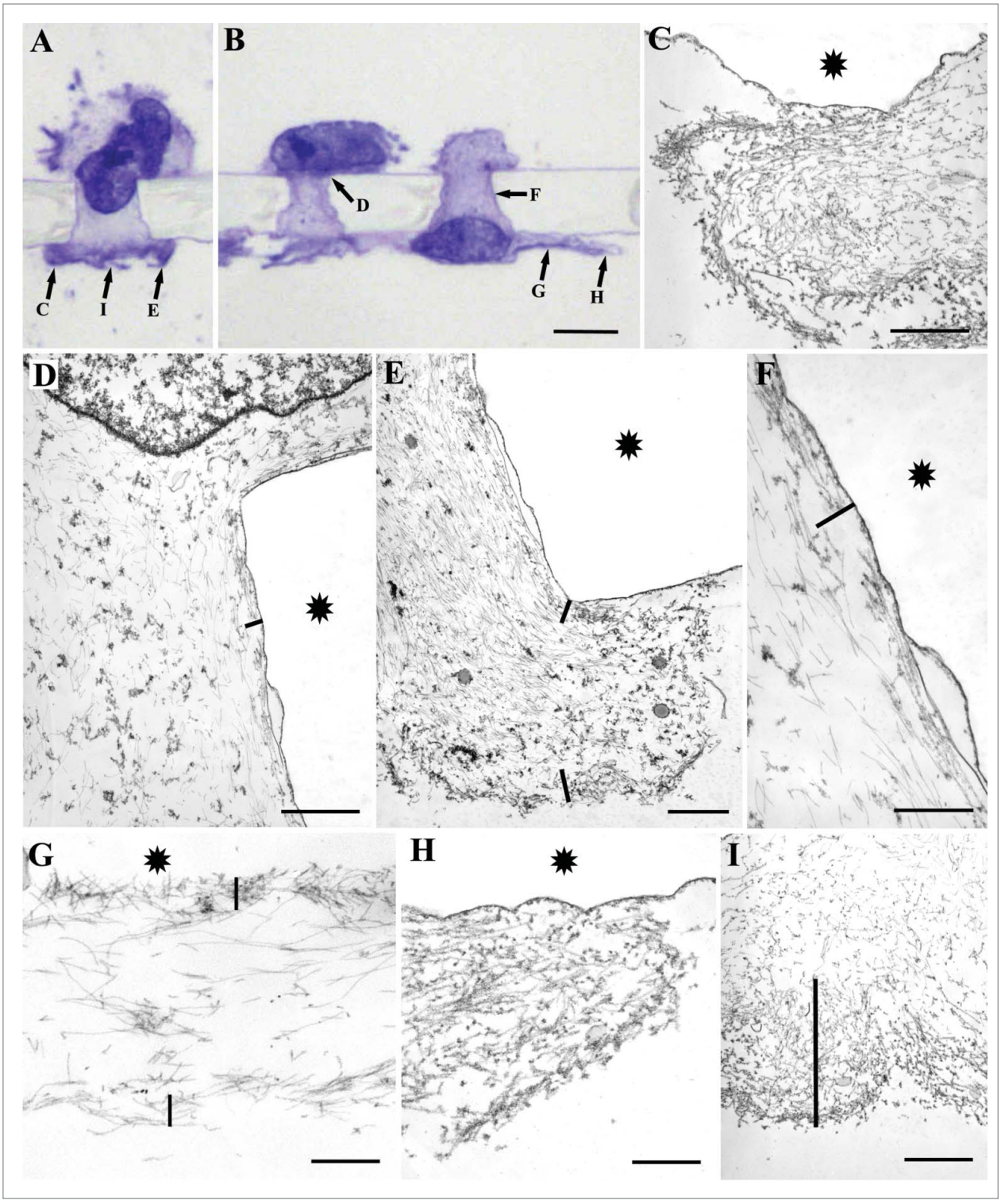

Figure 4. Electron microscopic images of HT1080 cells in the process of migration decorated with HMM to demonstrate the localization of actin filaments at ultrastructural level. The top of the micrographs correspond to the upper side of the filter. (**A and B**) Semithin sections of cells, which are in different phases of migration. Arrows with letters point at different parts of the cells shown on the electron micrographs. Asterisk indicates the localization of the filter. Bars show the approximate thickness of the cortical layer rich in actin filaments. Micrographs (**C and H**) show the leading edge of the migrating cells tightly packed with actin filaments. Other parts of the cells contain actin filaments of different thickness beneath the cell membrane (**D, E, F, G, and I**). The thickness of the actin filaments is the smallest under the membrane located within the pore (**D–F**). Undecorated filaments are intermediate (vimentin) filaments. Scale bars: (**A and B**) 10 μm, (**C, D, E, and I**) 1 μm, (**F–H**) 0.5 μm.

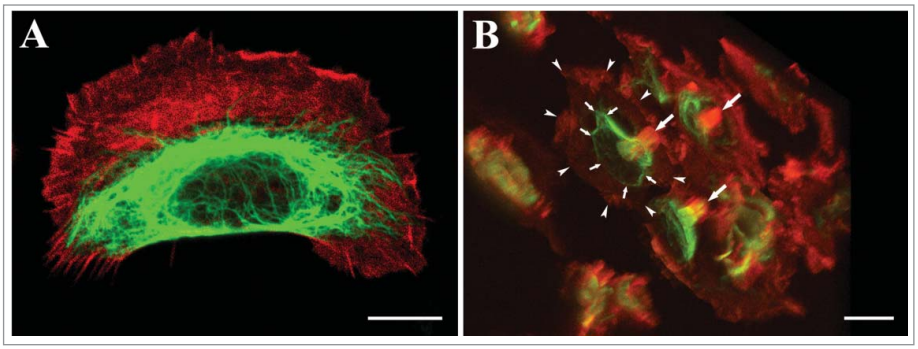

Figure 5. Arrangement of vimentin and actin filaments in 2D (**A**) and 3D (**B**) model systems. (**A**) Vimentin filaments enwrap the cell nucleus and are located behind the actin-rich leading lamella. Scale bar: (**A**) 10 μm. (**B**) Bottom side of the filter reconstructed from 30 optical sections and viewed from a 45 degree angle. The filter was stained for vimentin and filamentous actin. Three cells (large arrows) are clearly visible at the finishing stage of the migration through the filter. The large arrows also point at the pore of the filter through which the cells migrate. A part of the cell body is still within the pore. Small arrowheads point at the actin-containing largest extension of the cell. Small arrows point at the extension of the vimentin filament network at the bottom of the filter. Note the difference in the area covered by the two cytoskeletal elements. Scale bar: (**B**) 20 μm.

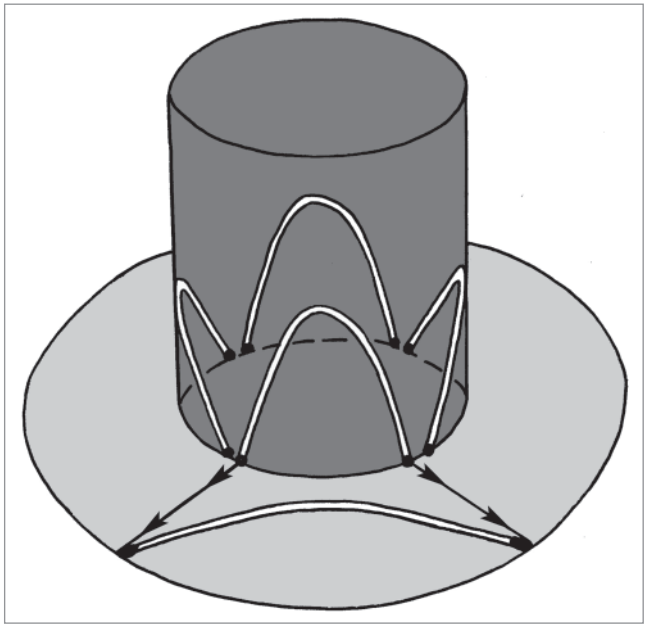

Figure 6. Schematic representation of the fate of adhesions and actin cables in moving cells within the 3D model system. The dark gray area represents the hole through which the cell migrates and the cell itself within the hole. Light gray color represents the area covered by the cell spreading on the bottom surface of the filter. White arcs are the actin cables, black dots are the adhesion sites, and the arrows show their path. Actin cables in the dark gray area are located within the cell, the front of which is situated at the bottom rim of the filter. The contractile force of the actin arcs connected to the adhesions at the front edge of the cell leads to cell body translocation. When the cell passes the rim of the hole, its actin arcs start to increase in length, and the adhesions at the end of the arcs move in a straight line. The actin cables maintain their arcs' form and the force exerted by them pulls the cell out of the hole.

Migration assay

Migration (chemotaxis) assays were performed in a 48-well-modified Boyden chamber (Neuroprobe) on 10 μm-thick uncoated Nucleopore membrane (Neuroprobe) with a pore diameter of 8 μm. Reconstituted fibronectin (50 μg/ml Sigma), Matrigel, and Collagen I (100 μg/ml, BD Biosciences) were used as chemoattractants, diluted in PBS (27.5 μl/well). A total volume of 50 μl of the applied cell suspensions (in medium containing 1% FCS) was placed in each well on the upper part of the chamber at a concentration 2×10^5/ml. Cells were incubated for 20–45 min at 37°C in 5% CO_2 atmosphere after the assembly of the chamber to achieve a sufficient number of cells within the pore or just reaching the lower surface of the filter at the termination of the experiment. The LX2 cell line was allowed to migrate 90 min and fibronectin (50 μg/ml, Sigma) was used as a chemoattractant.

Immunofluorescence

Following migration, cells, together with the membrane, were fixed in 4% paraformaldehyde for 10 min and permeabilized with 0.2% Triton X-100 for 5 min. After blocking with 3% BSA, the filters were incubated with anti-vinculin (mouse, clone VIN-11-5, Sigma, 1:20) and anti-vimentin (mouse, clone vim 3B4, DakoCytomation, 1:100) antibodies for 60 min. After washing, incubation with biotinylated secondary antibody (anti-mouse IGs, 1:100, Vector) and with streptavidin-Fluorescein (Vector Laboratories, 1:100) followed, each for 45 min. The antibodies were used in 1% BSA-PBS solution. Actin labeling was performed by tetramethylrhodamine (TRITC)—Phalloidin (1:500, 30 min, Sigma). Cells were then examined under confocal laser scanning microscopes (MRC 1024, BIO-RAD; NIKON Eclipse E6000, Nikon Optoteam).

Electron microscopy (HMM decoration)

Following the termination of the Boyden chamber migration assay, the filter was removed, washed with CSK buffer (20 mM HEPES, 3 mM $MgCl_2$, 50 mM KCl, 1 mM EDTA, pH 7), and extraction was performed with CSK solution containing 1% Triton X-100, 4% PEG, and 1:100 TRITC-phalloidin. Subsequently, HMM decoration was performed in TRIS-KCl solution containing 1 mg/ml HMM (30 min).

Samples were fixed in PBS containing 2.5% glutaraldehyde and 0.2% tannin for 30 min then submerged in 2% OsO_4 in PBS for 1 h. The specimens were dehydrated stepwise in alcohol: 50%, 75% (containing 2% uranyl acetate), 90%, 100%, then 30 min of 1:1 alcohol-resin mixture, finally incubated in Spurr's mixture, at 60°C for 24 h. The ultra-thin sections were contrasted with lead citrate and analyzed using an electron microscope (Philips CM10, FEI).

Conclusions

The present paper describes a model of the organization of adhesions and the cytoskeleton (actin and vimentin) of migrating cells in the Boyden chamber. The model is based on the observation that adhesions are present only at the leading edge of the cell. The path of the adhesions is unknown in the three-dimensional model studied (i.e., within the pore). Further study of the adhesion dynamics along with determination of the exact structure of the cytoskeleton is needed.

Disclosure of Potential Conflicts of Interest

No potential conflicts of interest were disclosed.

Acknowledgments

We kindly thank Katalin Derecskei for her excellent technical assistance. The LX2 spontaneously immortalized human hepatic stellate cell line was a kind gift from Dr Scott Friedmann for that the authors are very thankful.

Funding

This work was supported by the following grants: Hungarian Scientific Research Fund-OTKA K84173 (Tóvári J), PD109580 (Kenessey I); National Development Agency-NFU KTIA AIK 12-1-2013-0041 (Tóvári J), INNO 08-3-2009-0248 (Tóvári J).

Author Contributions

Tóvári J and Paku S designed the study. Tóvári J, Futosi K, and Paku S performed the migration assays. Bartal A, Gacs A, and Tátrai E performed the immunoassays. Tóvári J, Futosi K, Kenessey I, and Paku S performed the electronmicroscopy. Tátrai E, Bartal A, and Kenessey I drafted the manuscript. All authors read and approved the final manuscript.

References

1. Fraley SI, Feng Y, Krishnamurthy R, Kim DH, Celedon A, Longmore GD, Wirtz D. A distinctive role for focal adhesion proteins in three-dimensional cell motility. Nat Cell Biol 2010; 12:598-604; PMID:20473295; http://dx.doi.org/10.1038/ncb2062
2. Herant M, Dembo M. Form and function in cell motility: from fibroblasts to keratocytes. Biophys J 2010; 98:1408-17; PMID:20409459; http://dx.doi.org/10.1016/j.bpj.2009.12.4303
3. Lee J, Leonard M, Oliver T, Ishihara A, Jacobson K. Traction forces generated by locomoting keratocytes. J Cell Biol 1994; 127:1957-64; PMID:7806573; http://dx.doi.org/10.1083/jcb.127.6.1957
4. Mogilner A, Keren K. The shape of motile cells. Curr Biol 2009; 19:R762-71; PMID:19906578; http://dx.doi.org/10.1016/j.cub.2009.06.053
5. Verkhovsky AB, Svitkina TM, Borisy GG. Myosin II filament assemblies in the active lamella of fibroblasts: their morphogenesis and role in the formation of actin filament bundles. J Cell Biol 1995; 131:989-1002; PMID:7490299; http://dx.doi.org/10.1083/jcb.131.4.989
6. Theriot JA, Mitchison TJ. Actin microfilament dynamics in locomoting cells. Nature 1991; 352:126-31; PMID:2067574; http://dx.doi.org/10.1038/352126a0
7. Lee J, Ishihara A, Theriot JA, Jacobson K. Principles of locomotion for simple-shaped cells. Nature 1993; 362:167-71; PMID:8450887; http://dx.doi.org/10.1038/362167a0
8. Abercrombie M, Heaysman JE, Pegrum SM. The locomotion of fibroblasts in culture. I. Movements of the leading edge. Exp Cell Res 1970; 59:393-8; PMID:4907703; http://dx.doi.org/10.1016/0014-4827(70)90646-4
9. Cramer LP, Siebert M, Mitchison TJ. Identification of novel graded polarity actin filament bundles in locomoting heart fibroblasts: implications for the generation of motile force. J Cell Biol 1997; 136:1287-305; PMID:9087444; http://dx.doi.org/10.1083/jcb.136.6.1287
10. Paku S, Tóvári J, Lörincz Z, Timár F, Döme B, Kopper L, Raz A, Tímár J. Adhesion dynamics and cytoskeletal structure of gliding human fibrosarcoma cells: a hypothetical model of cell migration. Exp Cell Res 2003; 290:246-53; PMID:14567984; http://dx.doi.org/10.1016/S0014-4827(03)00334-3
11. Tayalia P, Mazur E, Mooney DJ. Controlled architectural and chemotactic studies of 3D cell migration. Biomaterials 2011; 32:2634-41; PMID:21237507; http://dx.doi.org/10.1016/j.biomaterials.2010.12.019
12. Niggemann B, Drell TL 4th, Joseph J, Weidt C, Lang K, Zaenker KS, Entschladen F. Tumor cell locomotion: differential dynamics of spontaneous and induced migration in a 3D collagen matrix. Exp Cell Res 2004; 298:178-87; PMID:15242772; http://dx.doi.org/10.1016/j.yexcr.2004.04.001
13. Geiger B, Bershadsky A. Assembly and mechanosensory function of focal contacts. Curr Opin Cell Biol 2001; 13:584-92; PMID:11544027; http://dx.doi.org/10.1016/S0955-0674(00)00255-6
14. Jockusch BM, Rüdiger M. Crosstalk between cell adhesion molecules: vinculin as a paradigm for regulation by conformation. Trends Cell Biol 1996; 6:311-5; PMID:15157439; http://dx.doi.org/10.1016/0962-8924(96)10022-2
15. Ziegler WH, Liddington RC, Critchley DR. The structure and regulation of vinculin. Trends Cell Biol 2006; 16:453-60; PMID:16893648; http://dx.doi.org/10.1016/j.tcb.2006.07.004
16. Humphries JD, Wang P, Streuli C, Geiger B, Humphries MJ, Ballestrem C. Vinculin controls focal adhesion formation by direct interactions with talin and actin. J Cell Biol 2007; 179:1043-57; PMID:18056416; http://dx.doi.org/10.1083/jcb.200703036
17. Mierke CT, Kollmannsberger P, Zitterbart DP, Smith J, Fabry B, Goldmann WH. Mechano-coupling and regulation of contractility by the vinculin tail domain. Biophys J 2008; 94:661-70; PMID:17890382; http://dx.doi.org/10.1529/biophysj.107.108472
18. Mierke CT, Kollmannsberger P, Zitterbart DP, Diez G, Koch TM, Marg S, Ziegler WH, Goldmann WH, Fabry B. Vinculin facilitates cell invasion into three-dimensional collagen matrices. J Biol Chem 2010; 285:13121-30; PMID:20181946; http://dx.doi.org/10.1074/jbc.M109.087171
19. Small JV, Geiger B, Kaverina I, Bershadsky A. How do microtubules guide migrating cells? Nat Rev Mol Cell Biol 2002; 3:957-64; PMID:12461561; http://dx.doi.org/10.1038/nrm971
20. Zaman MH, Trapani LM, Sieminski AL, Mackellar D, Gong H, Kamm RD, Wells A, Lauffenburger DA, Matsudaira P. Migration of tumor cells in 3D matrices is governed by matrix stiffness along with cell-matrix adhesion and proteolysis. Proc Natl Acad Sci U S A 2006; 103:10889-94; PMID:16832052; http://dx.doi.org/10.1073/pnas.0604460103
21. Wolf K, Alexander S, Schacht V, Coussens LM, von Andrian UH, van Rheenen J, Deryugina E, Friedl P. Collagen-based cell migration models in vitro and in vivo. Semin Cell Dev Biol 2009; 20:931-41; PMID:19682592; http://dx.doi.org/10.1016/j.semcdb.2009.08.005
22. Bravo-Cordero JJ, Hodgson L, Condeelis J. Directed cell invasion and migration during metastasis. Curr Opin Cell Biol 2012; 24:277-83; PMID:22209238; http://dx.doi.org/10.1016/j.ceb.2011.12.004
23. Baghy K, Dezső K, László V, Fullár A, Péterfia B, Paku S, Nagy P, Schaff Z, Iozzo RV, Kovalszky I. Ablation of the decorin gene enhances experimental hepatic fibrosis and impairs hepatic healing in mice. Lab Invest 2011; 91:439-51; PMID:20956977; http://dx.doi.org/10.1038/labinvest.2010.172
24. Xu L, Hui AY, Albanis E, Arthur MJ, O'Byrne SM, Blaner WS, Mukherjee P, Friedman SL, Eng FJ. Human hepatic stellate cell lines, LX-1 and LX-2: new tools for analysis of hepatic fibrosis. Gut 2005; 54:142-51; PMID:15591520; http://dx.doi.org/10.1136/gut.2004.042127